Journal of Materials Chemistry A

Accepted Manuscript

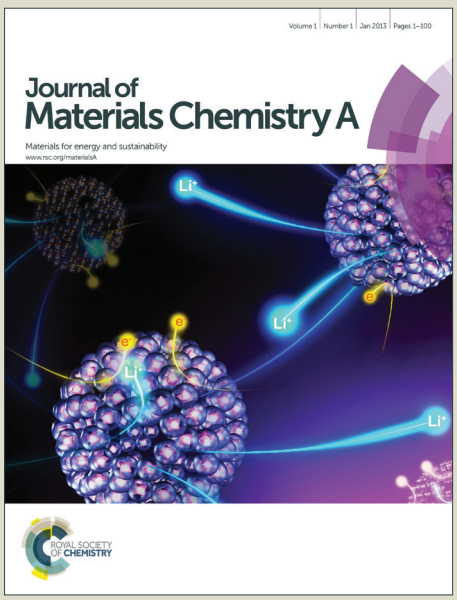

ROYAL SOCIETY OF CHEMISTRY

www.rsc.org/materialsA

Cite this: DOI: 10.1039/c0xx00000x

www.rsc.org/xxxxxx

ARTICLE TYPE

A facile two-step approach to prepare superhydrophobic surface on copper substrate

Huijie Wang, Jing Yu, Yizhi Wu, Weijia Shao and Xiaoliang Xu*

Received (in XXX, XXX) Xth XXXXXXXXX 20XX, Accepted Xth XXXXXXXXX 20XX

DOI: 10.1039/b000000x

Superhydrophobic surfaces were prepared on Cu substrates via a facile surface oxidation approach and subsequent chemical modification with low surface energy materials. In this paper, antiformin solution, as one of the most commonly used low cost disinfectants, is introduced for preparing bionic microstructure on copper surface for the first time. A short-time oxidation reaction soaking the Cu foil in antiformin liquid can result in the formation of a bean sprouts-like structure. Moreover, regulating the morphology of the microstructure can be realized by changing the reaction duration and solution concentration under a wide range of experimental conditions. A possible growth mechanism is also proposed here. After being modified by stearic acid, all as-etched surfaces possess superhydrophobic properties, with a water contact angle (CA) larger than 150° and a sliding angle (SA) less than 10°. Simultaneously superoleophobic interfaces can be obtained after the etched surfaces are modified with Heptadecafluorodecyltrimethoxy-silane (HTMS). The resultant samples present good thermal stability before the ambient temperature rises to 150 °C. The same approach is also suitable for brass materials. This offers an effective and practical route for large scale industrial production of superhydrophobic materials.

Introduction

Copper is a vitally important metal with extensive applications in daily life and industrial production for its mechanical plasticity, and high electrical and thermal conductivity. In recent years, superhydrophobic Cu surfaces with a contact angle (CA) greater than 150° have aroused wide concern because of their potential application prospects in self-cleaning, anticorrosion, oil-water separation, no loss transport of droplets, freezing-proof, and so forth[1-7]. Some phase transition process of the droplets on Cu-based hydrophobic surfaces have also been studied, such as droplet condensation[8], the generation of air bubbles[9], and evaporation of water droplets[10], etc. Inspired by a variety of functional interfaces with special wettability in nature such as lotus leaf, butterfly wings, or mosquito compound eyes, multifarious bionic microstructures including acicular, honeycomb-like, petal shaped, feathery, and network-like, and so forth, have been rendered on Cu and Cu alloy surfaces. [3, 11-14] This even includes a biomimetic water strider that can float on an interface of liquids[15] .

In general, the wettability of a solid surface is governed by both the surface chemical composition and geometrical microstructure. The chemical composition and atomic arrangements of a solid itself only can result in a limited increase in contact angle, and is insufficient to make a surface superhydrophobic. However, increasing surface roughness of hydrophobic materials can significantly enhance the surface's capacity to repel water [16].

Rough surfaces are generated by using "top-down" and "bottom-up" methods. The most common used "top-down" methods are "etching", such as plasma etching, and nano-imprinting photo- and electron-beam lithography[17-21]. By means of "etching", there is no obvious phase interface between the rough surface film and the substrate, and the hierarchical structures on the surface have the same phase as the substrate does. Thus, such superhydrophobic surfaces possess superior mechanical stability. However, "top-down" approaches are time consuming and expensive due to some experimental facilities such as lithography and plasma etcher. So far, a series of "bottom-up" techniques have been applied to prepare artificial superhydrophobic Cu surfaces for the simple and fast process.[2, 13, 22-28] The related methods include electroless galvanolysis deposition, electrostatic deposition, sol-gel, ion-exchange, thermal oxidation, and template assisted, growth of another phase on a Cu substrate, and so on.

In this study, the antiformin solution is introduced to prepare CuO microstructure on Cu surfaces because of the strong oxidizing property of hypochlorite anion (ClO^-). Multifarious microstructures have been obtained by changing the reaction duration and solution concentration. The growth threshold of CuO nanowires is also researched. As-etched surfaces are endowed with superhydrophobic property or superoleophobic property by being modified with stearic acid or Heptadecafluorodecyltrimethoxy-silane (HTMS), respectively. The thermal stability of superhydrophobic interfaces has been systematically investigated. The present approach could be readily used to create large area superhydrophobic materials because this procedure is carried out in an available and economical aqueous solution, which is fairly facile to operate and

no special technique or equipment is required. Also, it can also be generalized to other metal substrate, for example brass materials.

Experiment

Materials and Reagents

Cu foil (0.1mm thick, 3N), antiformin (CP, free alkali 7.0~8.0%, active chlorine≥5.2%), stearic acid (AR), hydrochloric acid (36%~38%), acetone (AR), ethanol (AR), isopropanol (AR) were used in the experiment. All reagents were bought from Sinopharm Chemical Regent Co. Ltd. (Shanghai, China). Brass foil, alloy 260, 0.25mm (0.01 in) thick was acquired from Alfa Aesar. Heptadecafluorodecyltrimethoxy-silane ($C_{13}F_{17}H_{13}O_3Si$, HTMS) was bought from Dow Corning Co. (USA). Deionized water with resistivity 18.25 MΩ·cm was used in the whole experimental process.

Experiment details

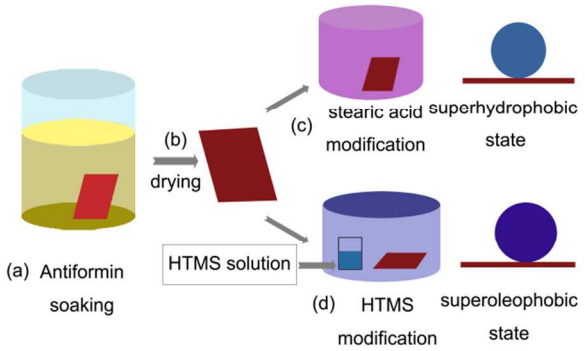

Scheme 1 Schematic illustration of the main route used to prepare superhydrophobic surface on Cu substrate.

In a typical procedure, Cu foils were first ultrasonically cleaned in acetone, ethanol, and deionized water for 5 min, respectively, then dipped in 1 M sulphuric acid for 20 s to remove surface oxides, rinsed with water and ethanol, and dried with a stream of nitrogen. The main process to fabricate superhydrophobic copper surfaces is shown in Scheme 1. Two kinds of reaction solutions were mainly prepared for copper corrosion: one solution was prepared by diluting 30 mL antiformin solution to 100 ml with deionized water, namely 30% volume fraction (VF), the other one was prepared by diluting 20 mL antiformin solution to 100 ml with deionized water, namely 20% volume fraction (VF). Cleaned Cu foils were immersed in antiformin solution at room temperature (Fig.1a). The reaction duration in solution with 30% VF and 20% VF was consistent from 15 s to 20 min. After thoroughly washed with deionized water and ethanol, samples were dried under a heat blower with temperature about 70 °C (Fig.1b). Consequently, cupric oxide films formed on the substrates. The etched samples were modified by 0.01 M stearic acid solution (the solvent is ethanol) for 15 min to lower the surface energy. The whole experimental process took less than one hour (Fig.1c). In addition, an oleophobic surface could be achieved through HTMS modification by a thermal evaporation process as follows: as-etched specimens and a bottle of 1mL HTMS solution (5 Vol %, the solvent is isopropanol) were sealed in a glass container, and placed in an oven at 85 °C for 3 h to reduce the surface energy (Fig.1d).

Based on the same approach, as-cleaned brass sheets were directly dipped in 100% VF and 20% VF antiformin solution, the reaction duration is 1 min and 5 min respectively. As-etched samples were modified in 0.01 M stearic acid ethanol solution for 40 min.

Characterization

The morphologies of the samples were observed using field emission scanning electron microscopy (FESEM, JSM-6700F), and the operating voltage is 5kV. The phase structure of the as-prepared samples was characterized by an X-ray diffractometer (XRD) (PHILIPS Corp., X'Pert PRO) using Cu-Kα radiation (λ=0.154 nm). The scanning angle ranges from 20° to 80° and the grazing-incidence angle is 2°. The surface chemical component was analysed by an X-ray photoelectron spectroscope (XPS) (THERMO Corp., ESCALAB250) equipped with a standard monochromatic Al-Kα radiation (hν=8047.8 eV), the test depth is 3 nm. The static water contact angle (CA) and sliding angle (SA) were measured by the CAST2.0 contact angle analysis system (Solon Information Technology Co. Ltd., Shanghai, China) in ambient atmosphere. The volume of the individual water droplet used for the static CA and SA measurements was 4μL. And the average CA came from the measure of five different positions on the same sample. The contact angle hysteresis (CAH) was measured by holding the water droplet with a stationary needle in contact with the water surface and moving the goniometer stage in one direction. Related approach can be found elsewhere[11, 29]. For oily liquids contact angle (OCA) and SA measurement, formamide and diiodomethane have been used. The liquid droplet volume for the test is 2μL and 1μL, respectively.

Results and Discussion

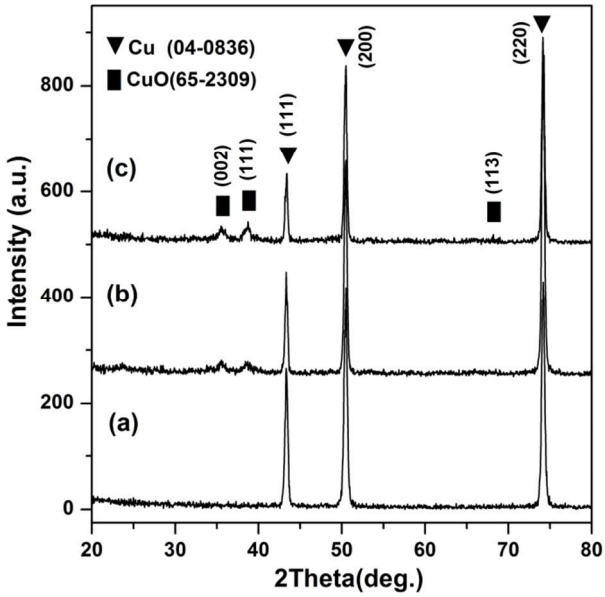

Fig. 1 XRD patterns of samples: (a) untreated copper foil, (b) after 10 min corrosion in 20% VF solution, and (c) after 10 min corrosion in 30% VF solution.

X-ray diffraction (XRD) analysis is used to determine the crystal structure. As a comparison, the XRD pattern of the Cu substrate

is recorded as depicted in Fig.1a, it only contains a cubic copper phase with lattice parameters of a=b=c=0.3615 nm (JCPDS no.04-0836 and ICSD #52256). After dipped in antiformin solution for 10 min, it shows that CuO is generated on the top layer of Cu substrate from Fig.1b and Fig.1c, and the CuO peaks are corresponding to (002), (111) and (113) crystallographic planes according to JCPDS no.65-2309 and ICSD #26715. Also a tendency can be found, with the increase of solution concentration from 20% VF (Fig.1b) to 30% VF (Fig.1c), the CuO diffraction peaks become more acute. The generation of CuO originates from the strong oxidizing property of ClO^- in an antiformin solution, and the reaction processes can be formulated as follows:

$$Cu + ClO^- \rightarrow CuO + Cl^-$$

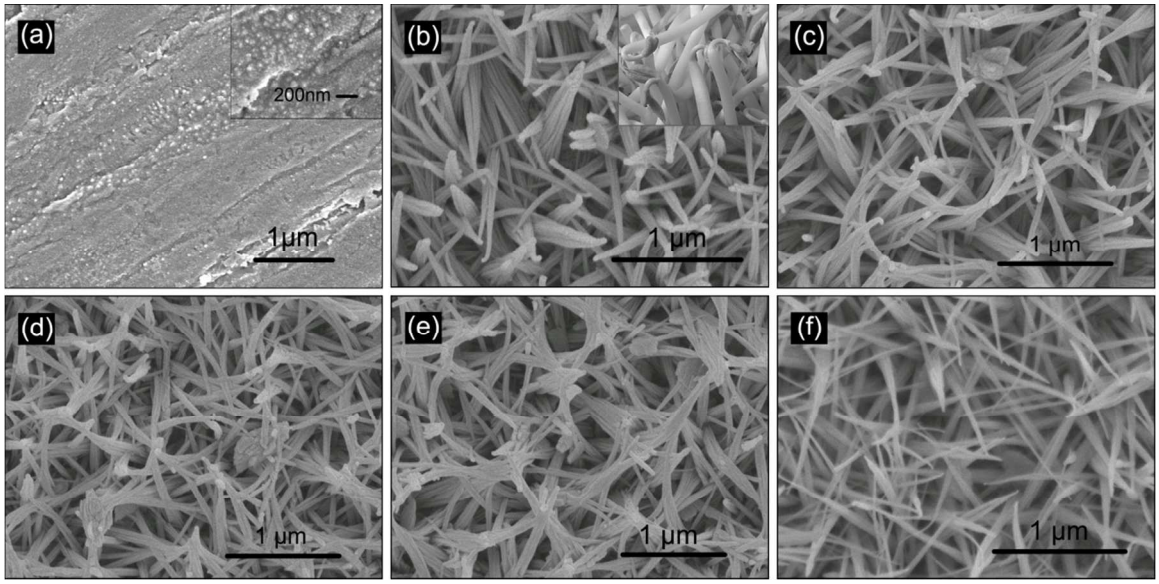

Fig. 2 FE-SEM images of CuO films prepared in 20% VF solution for different reaction durations: (a) 0 s, (b) 15 s, (c)(f) 1 min, (d) 5 min, and (e) 20 min. Samples corresponding to (b)-(e) are dried under heat flower, and sample corresponding (f) is dried under ambient temperature. The inset in (b) is bean sprout image.

The CuO microstructures during the whole immersion process have been carefully monitored. Fig.2 shows the FESEM images of the sample surfaces after immersing Cu substrate in the 20% VF antiformin solution for (a) 0 s, (b) 30 s, (c) (f) 1 min, (d) 5 min, (e) 20 min. Fig.2a depicts the original morphology of the Cu surface. Apart from a series of paralleled grains as a result of mechanical polishing, the surface is covered with promontories with size of about several tens of nanometers, which can be regarded as point defects (from the inset). When the immersion time is as short as 15 s, upward pine-like nanoneedles, with length in micro order and diameter of about tens of nanometers, are covering the whole region of the Cu substrate from Fig.2b. At a deeper level of observation, it shows that all nanoneedles are bundle structures composed of many thinner nanowires with diameter from 10 to 30 nm. Excitingly, a lot of nanoneedles possess bending tips, which is a typical bean sprouts-like microstructure（from the inset）. By extending the reaction time (1 min), nanowires start to become inclined and intertwined with each other (Fig.2c). After a 5 min reaction, nanowires are bending further, simultaneously some olive-like nanostructures are generated among the nanowires (Fig.2d). As the reaction time is prolonged to 20 min, nanowires become interconnected at the top and a reticular structure forms (Fig.2e). To clarify the growth mechanism of nanowires, a contrast sample has been prepared. Fig.2f is the FESEM image of Cu foil corroded in 20% VF solution for 1 min, the difference being that the sample is naturally drying, without any heating. In the micrograph, the bending degree of the nanoneedles is reduced greatly.

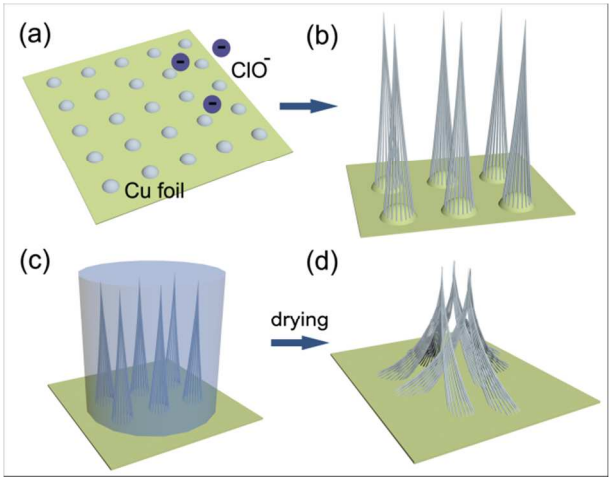

Fig. 3 The possible growth mechanism for nanowires in 20% VF solution

For 20% VF solution, time extension gives rise to the nanowires transitioning from individualization to collectivization. A possible growth mechanism is shown in Fig.3: firstly, the CuO nuclei forms on the protuberances on the surface of the Cu substrate; then the following CuO growth from the nuclei results in the appearance of thinner needle-like nanostructures due to their anisotropic growth rate. As the CuO seed crystals are so dense that many nanowires grow together, the coarser nanowires with bundle structure formed (Fig.3a-3b), which is a result of an aggregation effect caused by the liquid surface tension. The subsequent growth is explained by the tension junction model

that can be referred elsewhere[30]. Briefly, the result originates from the centripetal surface tension of the liquid: under high temperature flowing air, the liquid droplets existing among CuO nanowires evaporate and contract rapidly to form tiny drops, making the nanowires to be bent and aggregated. This process is depicted in Fig.3c-3d. For the antiformin solution with lower concentration, as the reaction time is extended, more and more CuO nanowires with a larger aspect ratio and smaller diameter appeared. They were more susceptible to be bent and assembled to form a reticulate structure. For any given diameter and density, nanowires would not overcome their own elastic modulus and assemble, but assembling by liquid surface tension would become prominent as the nanowires grew longer and thinner. This also can explain the bent tip of the sprouts-like structure.

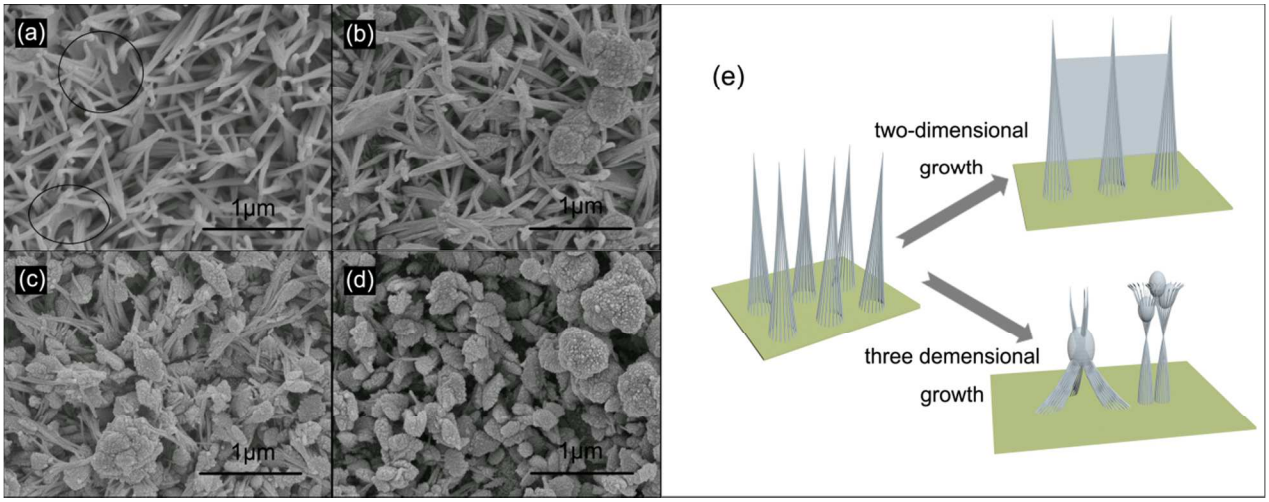

Fig. 4 FE-SEM images of CuO films prepared in 30% VF solution and the reaction mechanism diagram. The reaction time is: (a) 30 s, (b) 2 min, (c) 10 min, and (d) 20 min. (e) is the growth mechanism diagram.

Fig.4 is typical FESEM images of a CuO microstructure after immersing Cu substrate in 30% VF antiformin solution for different reaction durations. It seems that increasing the concentration of antiformin solution contributes to boosting the growth of two-dimensional and three-dimensional CuO microstructures from Fig.4a to 4d. In the initial stage of reaction (30 s), a nanoneedle-like structure and bean sprouts-like configuration are also obvious (Fig.4a), simultaneously some two-dimensional nano-sheets grow between the nanowires. Increasing the immersion time to 2 min, some thick nanowires begin to emerge, as well as some microspheres with rough surfaces (Fig.4b). With the increase of immersion time, spindle shaped and spherical microstructures grow more and more on the top of single nanoneedle or a group of nanoneedles. Also some nanowires grow through the three-dimensional nanostructures. Fig.4c reveals the morphology after 10 min corrosion. Further increasing the immersion time to 20 min, nanowires disappear from our view. As a replacement, microspheres and spindle structures with secondary nano papillary configuration achieve the full cover of the surface (Fig.4d), which is very similar to the hierarchical papillary structure of a lotus leaf.

For 30% VF solution, the possible growth mechanism for CuO architectures is depicted in Fig.4e. At the initial stage, CuO has a prior upwards growth tendency based on the protuberances on the Cu surface, which results in the formation of nanowires. On the position nanowires grow densely, CuO grows between adjacent nanowires, leading to the generation of nano-sheets. Compared with one-dimensional nanowires growth and two-dimensional nano-sheets growth, three-dimensional growth gradually shows its advantage. As nanowires grow longer, there is a larger probability for nanowires to interlace and aggregate with each other, especially on the tips as discussed above. These

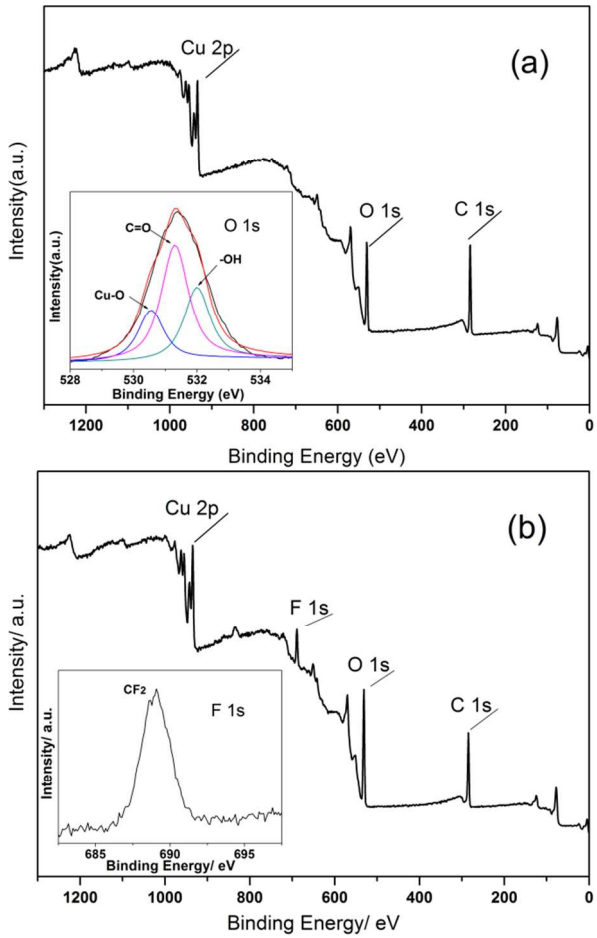

Fig. 5 XPS spectrum for modified surface: (a) stearic acid modified surface, the inset is the decomposed spectra of O 1s; (b) HTMS modified surface, the inset is spectrum of F 1s.

intersections provide prior locations for CuO growing. Meanwhile, some nanoneedles begin to bifurcate on the tip as depicted in Fig.4e, which contributes to the CuO cluster growth. As a result, three-dimensional structures formed, such as spherical or olive-like clusters with a secondary nanostructure.

In brief, controlling reaction duration is an effective approach to modulate the morphology of CuO microstructure. For solution with 30% VF, extending the reaction time, the number of nanowires would gradually reduce, and simultaneously spherical and olive like nanostructures increased. CuO microtopography will turn from a bean sprouts-like structure to a bionic lotus leaf structure. For the solution with 20% VF, time extension gives rise to the nanowires' transition from individualization to collectivization. By increasing the reaction time and solution concentration, the microstructure will transform from one dimension to three dimensions, from simple to complex. And concentration acts as a more important role.

XPS analysis is carried out to determine the surface chemical composition of the as-prepared CuO films modified by stearic acid and HTMS. Fig.5a shows the full spectrum of CuO film modified with stearic acid. To get more information about the surface composition, we collected high-resolution XPS data for O 1s, as is shown in the inset. The multielement spectra of O 1s is resolved into three components that centered at BE=530.5, 531.3, and 532 eV, which are ascribed to Cu-O, C=O, and -OH species, respectively[31-33]. All mentioned above chemical bonds reveal very thin layers of stearic acid molecules ($CH_3(CH_2)_{16}COOH$) have attached on the surface of the CuO film because the XPS investigation depth is only 3 nm under the specimen surface. Fig.5b shows the full spectrum of CuO film modified with HTMS. The inset shows the peak located at about 688.9 eV is ascribed to $-CF_2$ in the HTMS, which demonstrates that a stable monolayer of HTMS has already come into being on the surface of the CuO films by thermal evaporation process.

Table 1 Wettability measurement for samples reacted in 30% VF solution and 20% VF solution, the modification reagent is stearic acid.

Sample (30% VF)	AA/RA (°)	CA/SA (°)	Sample (20% VF)	AA/RA (°)	CA/SA (°)
15 s	158.5/156.7	158.0/3.5	15 s	159.0/156.0	157.0/5.0
30 s	161.2/159.6	159.8/1.5	30 s	158.1/151.2	153.8/7.0
1 min	163.3/162.0	162.4/1.2	1 min	162.0/154.1	155.5/7.5
2 min	164.1/160.3	161.8/4.4	2 min	158.0/152.5	155.1/5.8
5 min	162.3/154.1	155.2/7.5	5 min	162.0/158.0	152.6/4.8
10 min	160.8/155.4	157.0/6.6	10 min	162.2/158.6	158.8/3.2
20 min	161.0/156.1	158.0/3.0	20 min	159.6/155.3	156.4/4.4

Table 1 shows the results of CA, SA and CAH measurement for samples modified with stearic acid. The CAH value is the difference between Advanced Angle (AA) and Receding Angle (RA).The corresponding reaction duration is 15 s-20 min, respectively. There is no obvious incremental or diminishing tendency in the whole time interval for the CA. It indicates all samples present superhydrophobic property with CA larger than 150° and SA smaller than 10°. However, it is worth noting that The CAH values present the consistent change compared with the SA value, and the change rule is like a mechanical vibration curve (Fig.6). For 20% VF solution, the minimal value (3.0°) and maximum value (7.9°) appears at 15 s and 1 min. The state of water droplet on the surface belongs to Cassie State. From 15 s to 1 min, the nanowires get longer, becoming bent, increasing the contact area with liquid droplets. As a result, CAH increases. From 1 min to 10 min, bending the nanowires gradually aggregate at the tips, it seems a lot of papillae greatly reduce the contact area with water compared with just nanowires. A secondary minimum value appears at 10 min. However, enough reaction time (more than 10 min) also leads to the formation of two or three dimensional microstructures, which is similar with the situation of 30% VF solution.

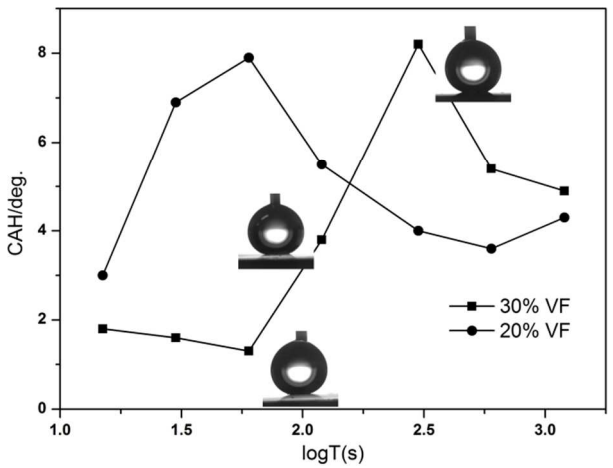

Fig. 6 CAH for stearic acid modified interfaces. The corresponding reaction duration in antiformin solution is 15 s, 30 s, 1 min, 2 min, 5 min, 10 min, and 20 min.

For 30% VF solution, the minimal value (1.3°) and maximum value (8.2°) appear at 1 min and 5 min respectively. The variation can be explained as follows: when the reaction time reaches 1 min from a shorter duration, large nanowires are generated, contributing to transition of water droplet state from Wenzel to Cassie state. The growth of nanowires is different from the

situation in 20% VF solution. As the reaction duration increases from 1 min to 5 min, large amounts of two or three dimensional microstructures form, mixed with nanowires, increasing the solid-liquid contact area, and giving rise to the increase of CAH. However, larger three dimensional hierarchical microstructures contribute to the transition of the configuration to a lotus structure, leading to the decrease of CAH.

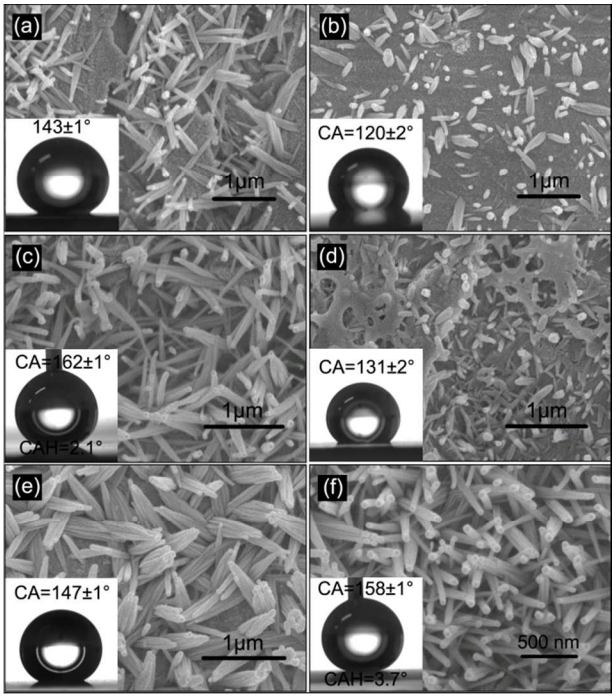

Fig. 7 Nanowires growth images in low concentration and short reaction duration, and the related hydrophobicity. (a) 5% VF, 15 s; (b) 10% VF, 8 s; (c) 10% VF, 15 s; (d) 30% VF, 1-2 s; (e) 30% VF, 5 s; and (f) 30% VF, 15 s.

It has been found nanowires can form in a lower concentration solution and shorter reaction duration, and hydrophobic property can be acquired. Fig.7a shows the surface configuration when the solution concentration is 5% VF and reaction time is 15 s, most of the area is covered with nanowires, with an average CA=143°. In a 10% VF solution, nanowire growth is faster, many nanowires appear after 8 s reaction, but the distribution is sparse (Fig.7b), with poor hydrophobicity. A bean-sprout like microstructure forms in 15 s and superhydrophobic interface has been acquired with AA/RA =162.9°/160.8°. In 30% VF solution, shorter nanowires would quickly form in 1-2 s, as depicted in Fig.6d, distinct nanoneedle bundles start to form in 5 s reaction duration, contributing to a CA 147°. As the immersion time reaches 10 s, a sprout-like structure begins to appear and superhydrophobic interface is acquired. The above mentioned results imply solution concentration acts a more important role in nanowire formation, 1 s is enough for nanowires to form in high VF solution, nanowire can appear in a 8 s duration in 10% VF solution, and 15 s may be a threshold to form a sprout-like structure in this concentration. However, to acquire a superhydrophobic interface, the Cu surface needs to be in full contact with a solution, and a 15 s reaction is also necessary.

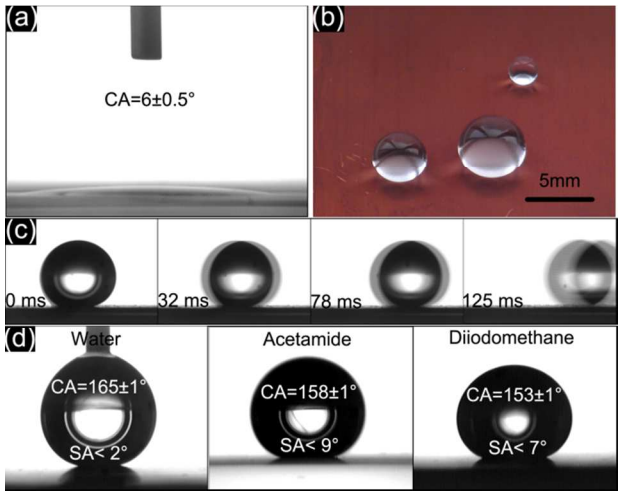

Fig. 8 Surface topography and surface wetting image for as-prepared sample. (a) The wetting state of water droplet on unmodified surface, (b) Macroscopic image for stearic acid modified surface, (c) the rolling of water droplet on stearic acid modified surface, and (d) the CA images for different liquid droplets on HTMS modified surface.

The macroscopic image for as-prepared Cu foil sample corroded in solution with 30% VF for 2 min is shown in Fig.8. A rough unmodified surface with CuO microstructure is superhydrophilic because of the large roughness. Fig.8a shows the wetting state of water droplet on unmodified surface, the CA is about 6°. Fig.8b depicts a reddish brown superhydrophobic surface can be acquired in a large area and the wetting state for water droplets with different diameters on a stearic acid modified surface, while all droplets keep good spherical shape. Fig.8c presents the rolling states of water droplets when inclining the sample stage. As the slant angle is larger than 5°, water droplets would slide, and quickly roll off. The wettability for different droplets on the HTMS modified surface is shown in Fig.8d. The CA for water droplets is 165°, larger than a corresponding stearic acid modified surface. Superoleophobic property has also been investigated, two kinds of oily liquids, formamide and diiodomethane, can roll off from the interface freely, with CA> 150°, SA< 10°.

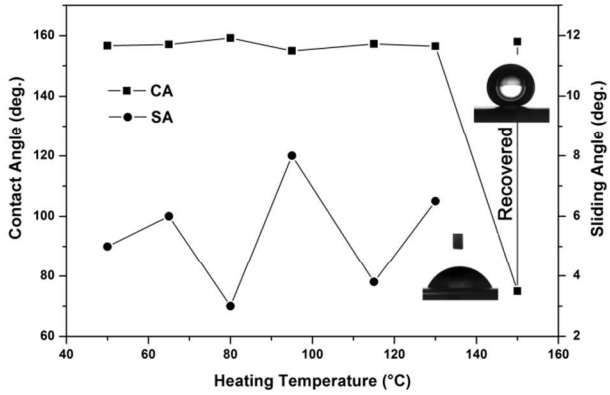

Fig. 9 Thermal stability test results for superhydrophobic surface.

To study the stability of the resultant samples in high temperature, a thermostatic drying oven was used to heat the specimens. Encouragingly, as-prepared superhydrophobic surfaces in solution with 30% VF for 2 min possess good stability in high temperature atmosphere. Fig.9 shows the anti-wetting state for water droplets on interfaces kept almost unchanged until

the ambient temperature exceeds 130 °C. Superhydrophobicity can be recovered by immersing the sample in stearic acid again. In addition, the superhydrophobicity can be kept as well after being dipped in water for 5 days. These above properties can be served as a promise for its practical application.

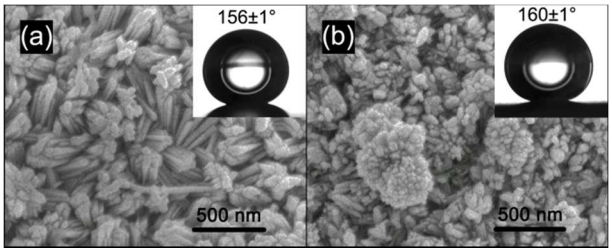

Fig. 10 Surface microstructure of brass corroded in antiformin solution and related CA images. (a) Corroded in solution with 20% VF for 5 min, (b) corroded in solution with 100% VF for 1 min.

The same method also can be applied on a Cu alloy, for example, brass (Cu-Zn alloy). Fig.8a shows the corrosion result after dipping the brass foil in a solution with 20% VF for 5 min. Clusters of nanorods in every direction cover the surface. As a comparison, 1 min immersion in 100% VF solution results in the generation of three dimension- spherical structures composed of secondary nanoparticles, which is very similar to the situation of copper (Fig.8b). It is thus clear that the concentration acts a more important role. Related wettability can be observed in the insets; both of the configurations present superhydrophobicity, especially for the lotus-like structure.

Conclusions

In summary, CuO microstructures with controlled morphology have been prepared on Cu surface by one-step oxidation with antiformin solution. With stearic acid or HTMS modification, all as-corroded surfaces possess excellent superhydrophobicity or superoleophobic property. Large area preparation has been realized. Simultaneously the anti-wet surface is endowed with good thermal stability. It offers superhydrophobic Cu and Cu alloy material a bright application prospect because this method owns a series of advantages such as available raw materials, time-saving, easy to operate and free of pollution.

Acknowledgement

We sincerely thank the National Natural Science Foundation of China (No. 51272246) and Scientific and Technological Research Foundation of Anhui (No. 12010202035) for financial support.

Notes and references

Department of Physics, University of Science and Technology of China, Hefei 230026, PR China. Tel: +86 551 63607574; E-mail: xlxu@ustc.edu.cn

1 A. Name, B. Name and C. Name, *Journal Title*, 2000, **35**, 3523; A. Name, B. Name and C. Name, *Journal Title*, 2000, **35**, 3523.

1. X. Zhu, Z. Zhang, X. Xu, X. Men, J. Yang, X. Zhou and Q. Xue, *J Colloid Interface Sci*, 2012, **367**, 443-449.
2. Z. Zhang, X. Zhu, J. Yang, X. Xu, X. Men and X. Zhou, *Applied Physics a-Materials Science & Processing*, 2012, **108**, 601-606.
3. L. Duc-Duong, N. Tuan Anh, L. Sungho, K. Jeong Won and K. Yong Shin, *Applied Surface Science*, 2011, **257**, 5705-5710.
4. S. J. Yuan, S. O. Pehkonen, B. Liang, Y. P. Ting, K. G. Neoh and E. T. Kang, *Corrosion Science*, 2011, **53**, 2738-2747.
5. J. Li, L. Shi, Y. Chen, Y. Zhang, Z. Guo, B.-l. Su and W. Liu, *Journal of Materials Chemistry*, 2012, **22**, 9774-9781.
6. Y. Xi, G. Jun, S. Yanlin and J. Lei, *Advanced Functional Materials*, 2011, **21**, 4270-4276.
7. H. Lingyan, L. Zhongliang, L. Yaomin and G. Yujun, *International Journal of Thermal Sciences*, 2011, **50**, 432-439.
8. J. Feng, Z. Qin and S. Yao, *Langmuir*, 2012, **28**, 6067-6075.
9. W. Xinwei, Z. Siwei, W. Hao and P. Tingrui, *Applied Thermal Engineering*, 2012, **35**, 112-119.
10. C. Y. Lee, B. J. Zhang, J. Park and K. J. Kim, *International Journal of Heat and Mass Transfer*, 2012, **55**, 2151-2159.
11. X. H. Chen, G. Bin Yang, L. H. Kong, D. Dong, L. G. Yu, J. M. Chen and P. Y. Zhang, *Crystal Growth & Design*, 2009, **9**, 2656-2661.
12. J. P. Liu, X. T. Huang, Y. Y. Li, K. M. Sulieman, X. He and F. L. Sun, *Journal of Materials Chemistry*, 2006, **16**, 4427-4434.
13. Z. She, Q. Li, Z. Wang, L. Li, F. Chen and J. Zhou, *Acs Applied Materials & Interfaces*, 2012, **4**, 4348-4356.
14. Q. M. Pan, H. Z. Jin and H. Wang, *Nanotechnology*, 2007, **18**.
15. X. Liu, J. Gao, Z. Xue, L. Chen, L. Lin, L. Jiang and S. Wang, *ACS Nano*, 2012, **6**, 5614-5620.
16. Z. X. Jiang, L. Geng and Y. D. Huang, *Journal of Physical Chemistry C*, 2010, **114**, 9370-9378.
17. J. Kim, P. Lin and W. S. Kim, *Thin Solid Films*, 2012, **520**, 4339-4343.
18. K. Ellinas, A. Tserepi and E. Gogolides, *Langmuir*, 2011, **27**, 3960-3969.
19. C. Bo, V. Sariola, S. Aura, R. H. A. Ras, M. Klonner, H. Lipsanen and Z. Quan, *Applied Physics Letters*, 2011, **99**.
20. X. Ye, Y. Duan, Y. Ding and H. Liu, *Journal of Vacuum Science & Technology A*, 2010, **28**, 564-567.
21. Y. Tian and L. Jiang, *Nat Mater*, 2013, **12**, 291-292.
22. G. Y. Wang and T. Y. Zhang, *Acs Applied Materials & Interfaces*, 2012, **4**, 273-279.
23. J. L. Song, W. J. Xu, Y. Lu and X. J. Fan, *Applied Surface Science*, 2011, **257**, 10910-10916.
24. P. Wang, D. Zhang and R. Qiu, *Applied Surface Science*, 2011, **257**, 8438-8442.
25. L. N. Pan, H. R. Dong and P. Y. Bi, *Applied Surface Science*, 2010, **257**, 1707-1711.
26. S. M. Lee, K. S. Kim, E. Pippel, S. Kim, J. H. Kim and H. J. Lee, *Journal of Physical Chemistry C*, 2012, **116**, 2781-2790.
27. J. Li, Z. Guo, J.-H. Liu and X.-J. Huang, *Journal of Physical Chemistry C*, 2011, **115**, 16934-16940.
28. Y. Huang, D. K. Sarkar and X. G. Chen, *Materials Letters*, 2010, **64**, 2722-2724.
29. D. K. Sarkar, M. Farzaneh and R. W. Paynter, *Materials Letters*, 2008, **62**, 1226-1229.

30. M. G. Gong, X. L. Xu, Z. Yang, Y. Y. Liu, H. F. Lv and L. Lv, *Nanotechnology*, 2009, **20**.
31. X. T. Zhu, Z. Z. Zhang, X. H. Men, J. Yang and X. H. Xu, *Acs Applied Materials & Interfaces*, 2010, **2**, 3636-3641.
32. T. Xu, S. Yang, J. Lu, Q. Xue, J. Li, W. Guo and Y. Sun, *Diamond and Related Materials*, 2001, **10**, 1441-1447.
33. X. M. Hou, F. Zhou, B. Yu and W. M. Liu, *Materials Science and Engineering a-Structural Materials Properties Microstructure and Processing*, 2007, **452**, 732-736.